

PITCHING AERODYNAMIC DAMPING IN A FREE FALL PHASE: BACKGROUND THEORIES AND NUMERICAL ANALYSES

*F. Paglia**, *D. Schiariti**, *R. Camussi***, *M. Gennaretti***, *F. Stella****, *M. Carta****, *R. Mancini*****

* *AVIO Spa, via Ariana km 5,2 – Colleferro (Rome), Italy, 00034*

** *Università Roma Tre, Dipartimento di Ingegneria, Via della Vasca Navale 79, 00146, Roma*

*** *Università Di Roma “La Sapienza”, Dipartimento di Ing. Meccanica e Aerospaziale
Via Eudossiana 18, 0084, Roma*

**** *ELV SpA, via degli esplosivi 1 - Colleferro (Rome), Italy, 00034*

Abstract

The present paper deals with the analysis of the aerodynamic damping of a fragment of a space launcher during a free fall phase. The work is focused on the estimation of the so called aerodynamic pitch damping coefficient, one of the most important quantity to be determined for the prediction of the spatial evolution and dynamics of a rigid body under free motion in the low altitude Earth atmosphere. A literature survey of the most important theories is presented as well as the general mathematical approach that starts from the governing equations of a 6dof rigid body and provides their simplified version for the purposes of engineering applications. According to classical approaches, in particular dealing with the application of the slender body theory, a discussion concerning the theoretical grounds of the software DATCOM shall be presented and its applicability limits outlined. A most reliable CFD methodology has been applied for a VEGA C LV fragment, in a phase where the motion is close to a stable attitude. In this configuration the body is subjected to damped oscillations associated to a periodic temporal evolution of the angle attack $\alpha(t)$, around the equilibrium position α_{eq} .

1. Introduction

The estimation of aerodynamic coefficients has been the subject of several theoretical, numerical and experimental studies, given the enormous importance in the field of fluid dynamics and flight dynamics. Attention has been focused on the study and analysis of the aerodynamic pitch damping coefficient of objects moving in a fluid, an old problem that has been faced since the early studies in the field of aviation at the beginning of the last century (e.g. Bryan, 1911). Fundamental theories can be found in reference textbooks treating aircraft flight mechanics (such as Etkin and Reid 1996) and dealing with missiles aerodynamics and design (e.g. Nielsen 1988, Chin 1961). To this extent, the most used approximation is the so-called Slender-body Theory, a simplified theoretical approach used for missile and airship design and a large body of literature has been devoted to this subject (including, among many, Munk 1924, Tsien 1938, Adams and Sears, 1953). More recent researches in literature, show that CFD is increasingly being used to create an aerodynamic database for aircraft configurations and axisymmetric flight bodies. It provides an accurate and efficient way to estimate the static stability derivatives since this involves steady-state simulations for a fixed geometry. The situation is different regarding the evaluation of dynamic derivatives since this involves unsteady simulations and/or moving geometries, thus decreasing the computational efficiency. However there is a strong need to improve CFD techniques for predicting dynamic derivatives, mainly for two reasons: a) wind tunnel tests are very expensive, time consuming and difficult to perform with the possible occurrence of blockage, scaling and Reynolds number effects; b) semi-empirical codes although having a low computational cost, provide reliable results only in a limited range of flow conditions. Navier-Stokes CFD solvers have reached a level of robustness and maturity to support the use of routine on relatively inexpensive computer clusters. The prediction of dynamic derivatives requires the ability to compute the aerodynamic response to time-dependent prescribed motions, which are used to excite the aerodynamics of interest. CFD has potential for complementing experimental testing techniques for obtaining these aerodynamic parameters. The physical limitations and kinematic restrictions of wind tunnel testing including model motion as well as the interference effects of the model support are not factors in the computational analysis. Physical effects can be separated from the CFD solutions in a way that can be difficult from

wind tunnel or flight test data. The purpose of this activity is to numerically evaluate the pitch damping coefficients in subsonic conditions for a fragmented configuration of Vega C. CFD analyses (using ANSYS Fluent) have been performed by simulating an unsteady pitching motion of the body around its center of gravity through the use of transient boundary conditions. This motion consists of small forced oscillations around a given equilibrium configuration. When this motion deals with large angles of attack and/or high frequencies the use of semi-empirical codes like MISSILE DATCOM (based on the “slender body theory”) provide unreliable results, so CFD analyses are required. A mesh sensitivity analysis has been performed in order to check the grid independence as well as simulations to study the influence of the time step size. A parametric analysis has been performed to study the influence of motion frequency on damping coefficients: this is important because it is hard to know the exact initial conditions for the free fall motion. The knowledge of aerodynamic damping coefficients is a key point to determine the stages’ re-entry trajectory in ordinary and extraordinary conditions (for example an unexpected explosion occurring during the lift-off phase).

2. Governing Equations

The definition of pitch aerodynamic damping derives from the mathematical model of governing equations for a 6 d.o.f. rigid body. These equations are relative to an inertial frame of reference but usually they are written in a moving frame of reference which is solidal with the body (“Body Frame of Reference”, BFR, see Figure 1). This is because in such reference system the moments of inertia are not depending on time, that is a clear advantage for calculations. Stability derivatives can be written in this frame of reference whose orientation with respect to a fixed system is given by Euler angles. The governing equations written in the BFR are:

$$\begin{cases} X = m(\dot{u} + qw - rv) \\ Y = m(\dot{v} + ru - pw) \\ Z = m(\dot{w} + pv - qu) \\ L = I_x \dot{p} + (I_z - I_y)qr - I_{xz}(pq + \dot{r}) \\ M = I_y \dot{q} + (I_x - I_z)rp - I_{xz}(p^2 - r^2) \\ N = I_z \dot{r} + (I_y - I_x)pq - I_{xz}(qr + \dot{p}) \end{cases}$$

where (u, v, w, p, q, r) and $(\dot{u}, \dot{v}, \dot{w}, \dot{p}, \dot{q}, \dot{r})$ represent the velocity and acceleration components respectively while forces and moments are given by (X, Y, Z, L, M, N) .

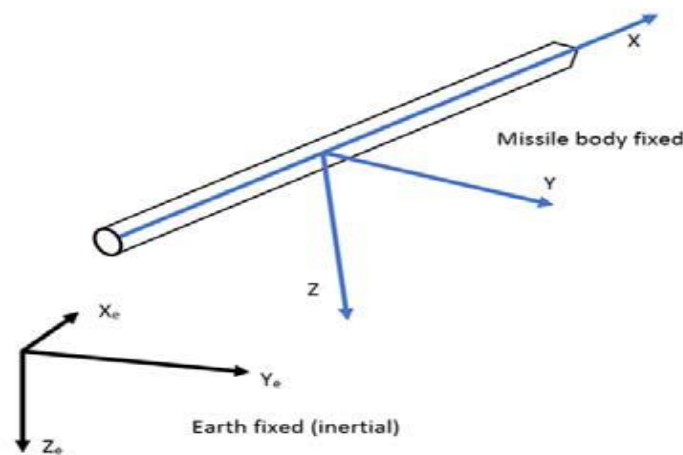


Figure 1: (B.F.R. and inertial frame of reference)

Such a model is simplified since it does not take into account the following effects: Coriolis force, Earth’s surface curvature and density variation with altitude. Since the aim of this work is to consider a body of revolution (that is axi-symmetric), the model described in previous equations can be reduced to a 3 d.o.f. system where only the c.o.g. (center of gravity) motion is considered. Furthermore, it is assumed that the pitching motion is independent from the c.o.g. motion (this hypothesis is acceptable when the frequency of pitching motion is high with respect to the c.o.g. velocity). In conclusion the only (scalar) equation that must be taken into account is the following one related to pitching motion:

$$M = I_y \dot{\theta} = I_y q$$

It is worth to underline that spin and ‘‘Magnus’’ effects are neglected as well as the presence of lateral forces, wind and gusts. The change of position of the center of pressure is not taken into account as well.

As a further clarification, in the following the theory of small perturbations around an equilibrium configuration is presented; the aim is to link the concepts of aerodynamic damping and dynamic stability. A Taylor series expansion truncated at first order is carried on, keeping in mind that aerodynamic forces are functionals depending not only on the actual value of state space variables but also from their time history. For slow motions it is reasonable to assume that forces and moments are a function only of the instantaneous dynamic state (represented by the components of velocity u, v, w, p, q, r), discarding accelerations.

For low values of α an expansion around t can be carried out:

$$\alpha(\tau) = \alpha(t) + \dot{\alpha}(t)(\tau - t) + \frac{1}{2} \ddot{\alpha}(t)(\tau - t)^2 + H.O.T.$$

So the pitching moment is:

$$M(t) = M[\alpha(t), \dot{\alpha}(t), \ddot{\alpha}(t) \dots]$$

If $M(t)$ is not a multivalued function, it is possible to expand in Taylor series around $t=0$. Then truncating at first order one obtains:

$$\Delta M := M(t) - M(0) \cong M_\alpha[\alpha(t) - \alpha(0)] + M_{\dot{\alpha}}[\dot{\alpha}(t) - \dot{\alpha}(0)] + M_{\ddot{\alpha}}[\ddot{\alpha}(t) - \ddot{\alpha}(0)]$$

where:

$$\begin{aligned} M_\alpha &:= \frac{\delta M}{\delta \alpha} \text{ at } \alpha = \alpha(0) \\ M_{\dot{\alpha}} &:= \frac{\delta M}{\delta \dot{\alpha}} \text{ at } \dot{\alpha} = \dot{\alpha}(0) \\ M_{\ddot{\alpha}} &:= \frac{\delta M}{\delta \ddot{\alpha}} \text{ at } \ddot{\alpha} = \ddot{\alpha}(0) \end{aligned}$$

If the body motion is slow enough, as said before, the third contribution related to the acceleration of α can be neglected, thus leading to this simple relationship:

$$\Delta M(t) \cong M_\alpha \Delta \alpha + M_{\dot{\alpha}} \Delta \dot{\alpha} + M_q \Delta q$$

where the contribution provided by pitch rate is also included. It is important to underline that ΔM is the perturbation term with respect to the reference condition and $M_q := \frac{\partial M}{\partial q}$. In the hypothesis of small perturbations the pitching equation can then be written as:

$$I_y \Delta \ddot{\theta} = \Delta M = M_\alpha \Delta \alpha + M_{\dot{\alpha}} \Delta \dot{\alpha} + M_q \Delta q$$

By introducing the definitions of M_α , $M_{\dot{\alpha}}$, M_q as well as the definition of moment coefficient, it is obtained:

$$I_y \Delta \ddot{\theta} = q_0 S_{REF} L_{REF} \frac{\delta C_m}{\delta \alpha} \Delta \alpha + q_0 S_{REF} L_{REF}^2 \frac{\delta C_m}{\delta \dot{\alpha}} \Delta \dot{\alpha} + q_0 S_{REF} L_{REF} \frac{\delta C_m}{\delta q} \Delta q$$

Where S_{REF} and L_{REF} are reference surface and length respectively. It is then possible to introduce the definitions of $\hat{q} := \frac{q L_{REF}}{2 V_0}$ and $\hat{\alpha} := \frac{L_{REF} \dot{\alpha}}{2 V_0}$ (respectively non-dimensional pitch rate and non-dimensional angle of attack) in order to render non dimensional all the derivatives that appear in:

$$I_y \Delta \ddot{\theta} = q_0 S_{REF} L_{REF} \frac{\delta C_m}{\delta \alpha} \Delta \alpha + \frac{q_0 S_{REF} L_{REF}^2}{2 V_0} \frac{\delta C_m}{\delta \hat{\alpha}} \Delta \hat{\alpha} + \frac{q_0 S_{REF} L_{REF}^2}{2 V_0} \frac{\delta C_m}{\delta \hat{q}} \Delta \hat{q}$$

The following quantities can be defined:

$$\begin{aligned} C_{m\alpha} &:= \frac{\delta C_m}{\delta \alpha} \\ C_{mq} &:= \frac{\delta C_m}{\delta \hat{q}} \end{aligned}$$

$$C_{m\dot{\alpha}} := \frac{\delta C_m}{\delta \dot{\alpha}}$$

By simply grouping the common terms at the right hand side, it becomes eventually:

$$I_y \Delta \ddot{\theta} = q_0 S_{REF} L_{REF} C_{m\alpha} \Delta \alpha + \frac{q_0 S_{REF} L_{REF}^2}{2V_0} (C_{m\dot{\alpha}} \Delta \dot{\alpha} + C_{mq} \Delta q)$$

It is fundamental to notice that the two quantities q , $\dot{\alpha}$ are different because they are related to two different type of motions. However in many applications where the trajectory of the body remains linear the condition $q = \dot{\alpha}$ is verified. Nevertheless the two quantities C_{mq} and $C_{m\dot{\alpha}}$ are not coincident also in rectilinear flight since they are stability derivatives and the physical interpretation remains different.

2. Datcom Approach

The ‘‘Slender Body Theory’’ was originally formulated by Munk [1] and Tsien [2] in order to evaluate the aerodynamic actions on bodies of revolution under the following basilar assumptions: ‘‘Slender’’ bodies and small angles of attack. The theory was then extended first by Multhopp [3] including the aerodynamic interaction with fuselage and then by Allen [4] who introduced the viscosity effects. First of all it is important to explain more clearly the meaning of the term ‘‘slender’’. Tsien stated that the theory is suitable for sharp projectiles in supersonic conditions. In fact the meaning of ‘‘slender’’ is deeply related to the flow regime conditions.

For supersonic flows a body is said to be ‘‘slender’’ if it ‘‘lies well’’ within the Mach cone that originates from the body’s tip (see Figure 2):

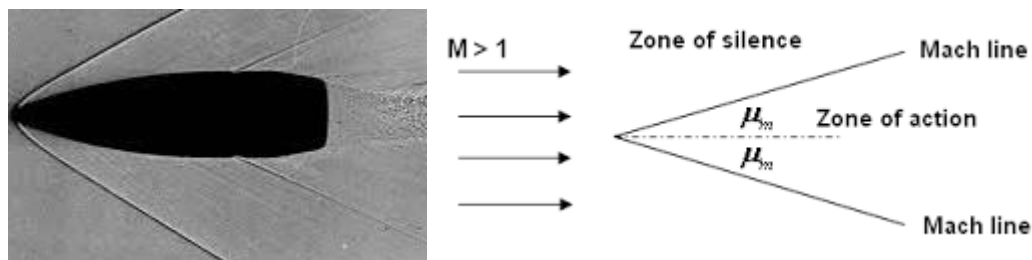


Figure 2: (Mach cone for a sharp projectile)

Such a definition apparently seems to restrict the range of application of the theory only to those bodies which own a sharp tip. Actually also ‘‘blunt bodies’’ can be regarded as ‘‘slender’’ for low supersonic regimes (so that the Mach cone span is large enough to contain the body). For subsonic regimes, as Mach number increases from 0 up to 1, the term ‘‘slender’’ becomes less restrictive until, for Mach=1, all bodies are slender independently from the geometry. In summary the slender body theory works well for bodies of revolution whose longitudinal dimension L is much larger than the transversal one D (see Fig.3):

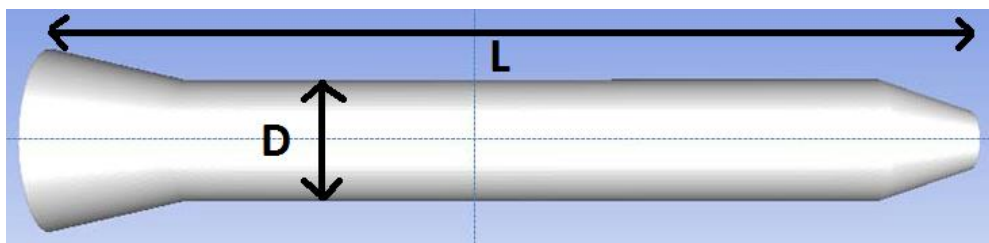


Figure 3: Example of a Slender Body with $L \gg D$

Or, equivalently speaking, the slenderness ratio defined as L/D is much greater than one:

$$\frac{L}{D} \gg 1 \quad \text{SLENDERNESS RATIO}$$

The starting point of the slender body theory is the potential equation written for compressible flows, both subsonic and supersonic. Since the flow is compressible such equation is not linear:

$$\left[a^2 - \left(V_0 + \frac{\delta\phi}{\delta x} \right)^2 \right] \frac{\delta^2\phi}{\delta x^2} + \left[a^2 - \left(\frac{\delta\phi}{\delta y} \right)^2 \right] \frac{\delta^2\phi}{\delta y^2} - 2 \left(V_0 + \frac{\delta\phi}{\delta x} \right) \frac{\delta\phi}{\delta y} \frac{\delta^2\phi}{\delta x \delta y} = 0$$

Where:

a : SPEED OF SOUND

ϕ : PERTURBATION POTENTIAL

The potential equation is then linearized in the hypothesis of small perturbations since, in the framework of the theory, the body is “slender” and the angle of attack is small. The linearized equation is:

$$(1 - M_\infty^2) \frac{\delta^2\phi}{\delta x^2} + \frac{\delta^2\phi}{\delta y^2} = 0$$

For slender bodies it is then possible to assume that, for an observer who is solidal with the body, the flow is the same on each plane orthogonal to the longitudinal axis x (see Figure 4):

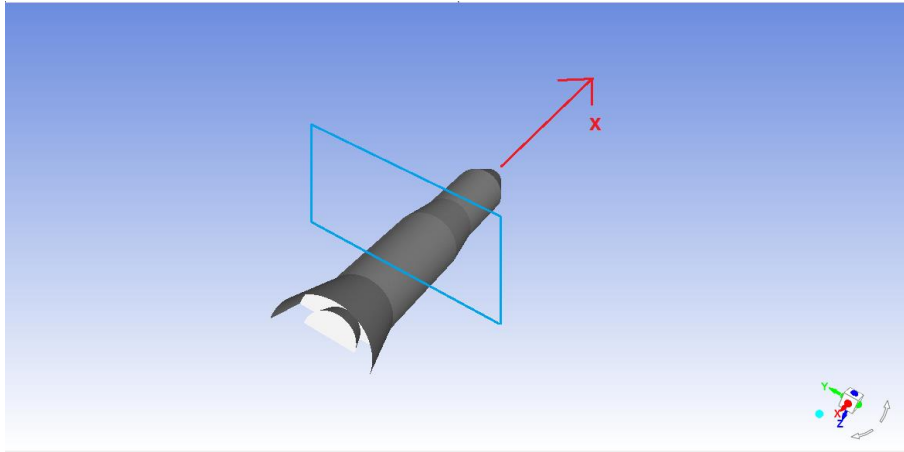


Figure 4: (Body cross plane)

So the following Laplace equation is valid on each plane yz :

$$\frac{\delta^2\phi}{\delta y^2} + \frac{\delta^2\phi}{\delta z^2} = 0$$

In order for this simplification to be valid the body must have a high slenderness ratio but it is also required that the longitudinal component of flow velocity is not subject to strong variations, therefore abrupt geometries are not allowed. The knowledge of the potential on each YZ plane allows to compute the velocity and the local force (“potential force”) $F_p(X)$ along the body [1]:

$$F_p(x) = (k_2 - k_1)q_0 \frac{dS}{dx} \text{sen}(2\alpha)$$

This force, for what said before, is only a function of the longitudinal dimension of the body and its dimensions are force per unit length. $S(x)$ is the cross-section area of the body while k_1 , k_2 are the longitudinal and transversal apparent mass coefficients. Since $F_p(x)$ derives from the potential theory it does not include the contribution of viscosity. It is then possible to add the effect of viscosity by including the force $F_v(x)$ [4]:

$$F_v(x) = 2\eta r(x)C_D q_0 \text{sen}^2 \alpha$$

where $r(x)$ is the body radius at any station x , C_D is the drag coefficient of an infinite circular cylinder as a function of Reynolds number, η is a correction factor that takes into account the body's finiteness. Finally also an axial viscous force can be added, $F_A(X)$ given by:

$$F_A(X) = C_{D\alpha=0} q_0 A \cos^2 \alpha$$

where A is the reference area for $C_{D\alpha=0}$. In summary the global force acting on the body is given by:

$$\vec{F}_{TOT}(X) = \vec{F}_p(X) + \vec{F}_v(X) + \vec{F}_A(X)$$

In Figure 5 it is reported a sketch of the body with the contribution of each force:

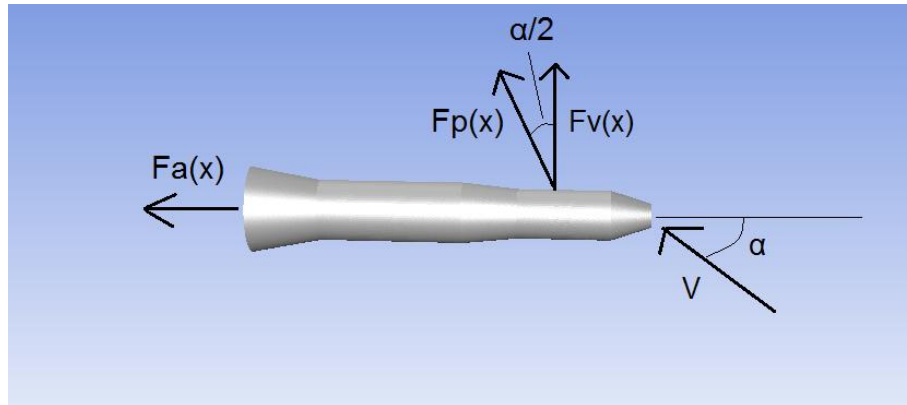


Figure 5: (Forces acting on the body)

By correctly projecting and integrating these contributions it is possible to compute drag, lift and moment (with respect to an arbitrary abscissa x_m):

$$D = (k_2 - k_1) q_0 \sin(2\alpha) \sin\left(\frac{\alpha}{2}\right) \int_0^L \frac{dS}{dx} dx + 2\eta q_0 \sin^2(\alpha) \sin(\alpha) \int_0^L r(x) C_D dx + C_{D\alpha=0} q_0 A \cos^2(\alpha) \cos(\alpha)$$

$$L = (k_2 - k_1) q_0 \sin(2\alpha) \cos\left(\frac{\alpha}{2}\right) \int_0^L \frac{dS}{dx} dx + 2\eta q_0 \sin^2(\alpha) \cos(\alpha) \int_0^L r(x) C_D dx - C_{D\alpha=0} q_0 A \cos^2(\alpha) \sin(\alpha)$$

$$M = (k_2 - k_1) q_0 \sin(2\alpha) \cos\left(\frac{\alpha}{2}\right) \int_0^L \frac{dS}{dx} (x_m - x) dx + 2\eta q_0 \sin^2(\alpha) \int_0^L r(x) C_D (x_m - x) dx$$

Before proceeding with calculations it is worth reminding that this formulation is valid only for low angles of attack (in particular $\alpha < 10^\circ$); furthermore the viscous term is only related to friction. Pressure drag is not included in the model and thus the contribution of flow separation to total drag cannot be considered.

For the purpose of the present work it is interesting to develop a simple expression for the aerodynamic moment by introducing two approximations:

$$(k_2 - k_1) \cong 1 \quad \text{for} \quad \frac{L}{D} \cong 10$$

The physical interpretation of coefficients k_1 , k_2 is related to the flow mass that is moved (both longitudinally and transversely) by the body during its motion. In other words a certain amount of energy is required to move the body as well as the flow around it. In particular below are reported the definitions of k_1 and k_2 , where V_b is the body volume:

$$k_1 = \frac{\text{FLUID VOLUME MOVED LONGITUDINALLY}}{V_b}$$

$$k_2 = \frac{\text{FLUID VOLUME MOVED TRANSVERSELY}}{V_b}$$

In addition :

$$\alpha \text{ small} \rightarrow \begin{cases} \text{sen}(\alpha) \cong \alpha \\ \text{cos}(\alpha) \cong 1 \end{cases}$$

The integrals that appear in the previous formula can be developed as follows:

$$\begin{aligned} \text{A) } & \int_0^L \frac{dS}{dx} dx = S_{REF} \\ \text{B) } & \int_0^L \frac{dS}{dx} (x_m - x) dx = V_b - S_{REF}(L - x_m) \end{aligned}$$

By introducing the moment coefficient C_m based on the body length L one obtains:

$$C_m \cong \frac{2\alpha}{S_{REF}L} [V_b - S_{REF}(L - x_m)] + o(\alpha^2)$$

It is evident how this theory allows to obtain a simple analytical expression for the functional relation $C_m(\alpha)$. By deriving with respect to α it is possible to obtain an expression for the derivative $C_{m\alpha}$ (based on S_{REF}, L):

$$C_{m\alpha} = 2 \left[\frac{x_m}{L} + \frac{V_b}{S_{REF}L} - 1 \right]$$

In a similar way an analytical expression for C_{mq} and $C_{m\dot{\alpha}}$ can be found:

$$\begin{aligned} C_{mq} &= 2 C_{m\alpha} \left[\frac{\left(1 - \frac{x_m}{L}\right)^2 - \frac{V_b}{S_{REF}L} \left(\frac{x_c}{L} - \frac{x_m}{L}\right)}{\left(1 - \frac{x_m}{L}\right) - \frac{V_b}{S_{REF}L}} \right] \\ C_{m\dot{\alpha}} &= 2 C_{m\alpha} \left[\frac{\frac{V_b}{S_{REF}L} \left(\frac{x_c}{L} - \frac{x_m}{L}\right)}{\left(1 - \frac{x_m}{L}\right) - \frac{V_b}{S_{REF}L}} \right] \end{aligned}$$

It is important to underline once again that these formulas lose validity for high angles of attack but also for high frequencies of motion since in this case the contribution of high order terms in reduced frequency cannot be neglected. These relations are actually the same used by DATCOM software to compute the damping coefficients .

3. Forced oscillations around an equilibrium position

Since the motion consists of small forced oscillations around an equilibrium configuration, the dynamic linear approach is suitable. This method, named Forced Oscillation Approach, has been extensively used in the past (see among many [7], [8], [9]) and is briefly worked out in the following. The problem can be studied as a classic forced harmonic oscillator; the body is forced to oscillate around an equilibrium angular position, in which: $\alpha = \alpha_{EQUILIBRIUM}$.

In the following analyses it is assumed that:

$$q = \dot{\alpha}$$

The oscillatory motion is imposed according to the following time-law:

$$\begin{cases} \alpha(t) = \alpha_{EQ} + \alpha_0 \sin \omega t \\ q(t) = \dot{\alpha}(t) = \omega \alpha_0 \cos \omega t \end{cases}$$

Where:

$\alpha(t)$: instantaneous angle of attack
 α_{EQ} : equilibrium angle of attack

ω : pitch frequency
 α_0 : oscillations amplitude

It is then possible to define the “reduced frequency” as follows:

$$k = \frac{\omega L_{REF}}{2 V_0}$$

The linearized expression for the moment coefficient around α_{EQ} is

$$C_m(\alpha(t)) = C_m(\alpha_{EQ}) + C_{m\alpha}\Delta\alpha + \frac{L_{REF}}{2V_0}(C_{mq} + C_{m\dot{\alpha}})\dot{\alpha}$$

Defining:

$$C_{mST} := C_m(\alpha_{EQ}) + C_{m\alpha}\Delta\alpha$$

and introducing C_{mEQ} , one obtains:

$$C_m(\alpha(t)) = C_{mST} + \frac{L_{REF}}{2V_0}C_{mEQ}\dot{\alpha}$$

It is possible to assume that C_{mEQ} is constant in a period so the previous equation can be integrated with respect to the angle of attack:

$$\overline{C_{mEQ}} = \frac{2 V_0}{L_{REF}} \frac{\int C_m(\alpha(t))d\alpha - \int C_{mST}d\alpha}{\int \dot{\alpha} d\alpha}$$

Since the integral of C_{mST} in one period is zero, that is:

$$\int_0^T C_{mST}d\alpha = 0$$

then :

$$\overline{C_{mEQ}} = \frac{2 V_0}{L_{REF}} \frac{\int C_m(\alpha(t))d\alpha}{\int \dot{\alpha} d\alpha}$$

It is convenient to change the integration variable, switching from α to t , and keeping in mind that:

$$\begin{cases} \alpha(t) = \alpha_{EQ} + \alpha_0 \sin \omega t \\ d\alpha = \omega \alpha_0 \cos \omega t dt \end{cases}$$

Finally one obtains:

$$\overline{C_{mEQ}} = \frac{2 V_0}{L_{REF} \pi \alpha_0} \int_0^T C_m(t) \cos \omega t dt$$

The integral can be evaluated numerically once the solution has reached a periodic steady-state condition. The time history of the moment coefficient can be easily obtained as an output of CFD analyses. This set must be referred to an entire period of oscillation, identified by a specific value of k through the following relation:

$$T = \frac{\pi}{k}$$

In a similar manner it is possible to compute the other longitudinal derivative $C_{N\text{EQUIVALENT}}$, defined as:

$$C_{N\text{EQUIVALENT}} := (C_{nq} + C_{n\dot{\alpha}})$$

and evaluated through:

$$\overline{C_{NEQ}} = \frac{2 V_0}{L_{REF} \pi \alpha_0} \int_0^T C_n(t) \cos \omega t dt$$

4. VEGA C CFD Analyses

Table 1 summarizes the input parameters for the CFD analyses in terms of frequency of motion, Mach number and corresponding reduced frequency:

Table 1: Angular velocity, Mach number and reduced frequency

$\omega(\text{rad/s})$	$M_\infty=0.6$
0.1	K=0.048
0.25	K=0.119
0.5	K=0.239
1.0	K=0.478
1.5	K=0.718
2.0	K=0.957

This parametric analysis is necessary because it is quite difficult to determine the exact initial conditions for the free fall motion. The pitching motion is simulated by using transient boundary conditions in which the angle of attack is changing in time. This relation can be written in terms of reduced frequency as follows:

$$\alpha(t) = \alpha_{EQ} + \alpha_0 \sin(2kt)$$

In Tab. 3.2 are reported the values of α_{EQ} and α_0 used for the analysis:

Table 2: Input values for oscillating motion

α_{EQ}	α_0
120	10

The value of α_{EQ} is a fixed input parameter for the current analysis. In Figure 6 is reported the $\alpha=0^\circ$ direction as well as the current angular equilibrium position.

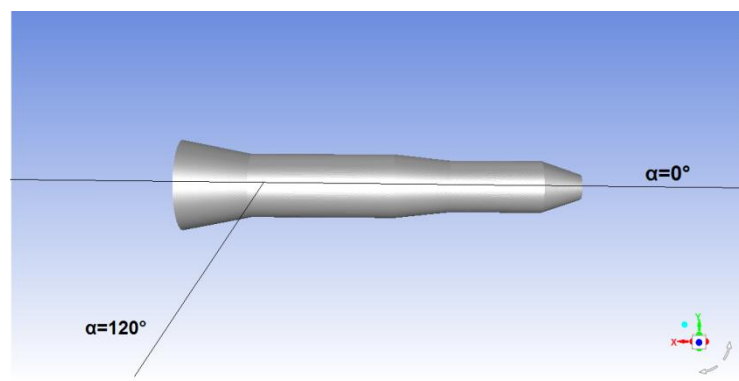


Figure 6: (Reference system for AoA)

4.1 Mesh Global features

The mesh used for calculations has been created with the software Gambit and its topology is reported in Figure 7. Only half body is built in the model in order to limit the computational cost; an appropriate symmetry plane

(symmetry boundary condition) is therefore included. The external domain is made up of four concentric semi-spheres whose radii ranges from 50 to 500m. The mesh is un-structured in the whole domain.

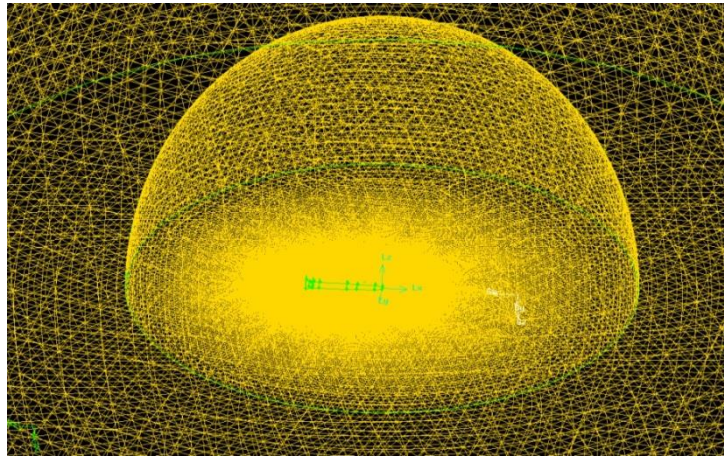


Figure 7: (Mesh topology)

4.2 Mesh Sensitivity

In order to check whether the results are grid independent it is essential to perform a mesh sensitivity analysis. Four progressively finer meshes have been created starting from the coarsest one (mesh A). Mesh refinements in the region around the body have been performed and their entity is qualitatively illustrated in Figure 8.

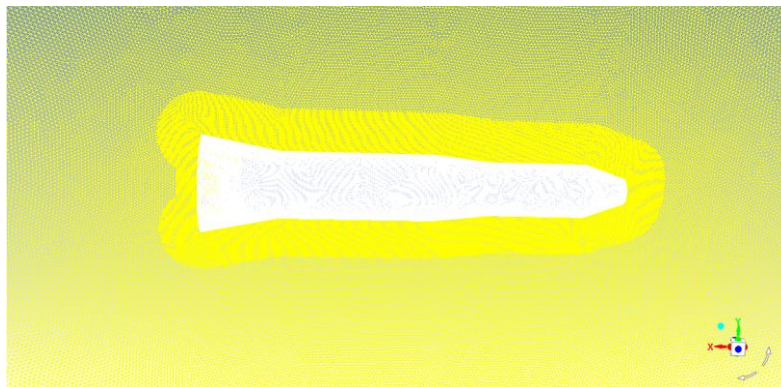


Figure 8: (Example of mesh refinement)

In Figure 9 is depicted the mesh in proximity of the body, pointing out the local cell size:

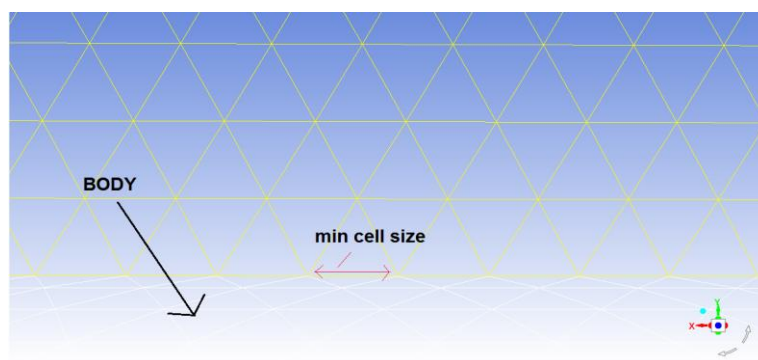


Figure 9: (Mesh size nearby the body wall)

Definitely, the global features of the four different meshes (mesh A, mesh B, mesh C, mesh D) are reported in Table 3.

Table 3: Global Mesh characteristics

Mesh	Cells	Min cell Size (mm)
A	884625	0.2
B	2612638	0.1
C	3775933	0.05
D	5002578	0.025

Once the solution is converged, it is important to focus on the last cycle of oscillation of the moment coefficient; this information is useful to compute the damping coefficients and to build a hysteresis loop by plotting such period as a function of the angle of attack. Hysteresis cycles are frequent phenomena in unsteady aerodynamics, especially when pitching oscillations are performed around the center of gravity. The presence of hysteresis cycles is linked to the combined effects of pitch rate q and $\dot{\alpha}$. The basic concept is that aerodynamic forces depend not only from the actual value of state variables (for example the angle of attack) but also from their time history. Hysteresis is, by definition, a dynamic lag between an input and an output. The presence of this “lag” is evident because the values of C_A , C_N and C_m at the same instantaneous angle of attack, between the downstroke and upstroke motions, are different. Hysteresis loops have been computed for both moment and normal force coefficients. In Figure 10 and Figure 11 are reported the hysteresis loops of moment coefficient and normal force coefficients evaluated referring to the last period of oscillations and for all the meshes considered in the analysis:

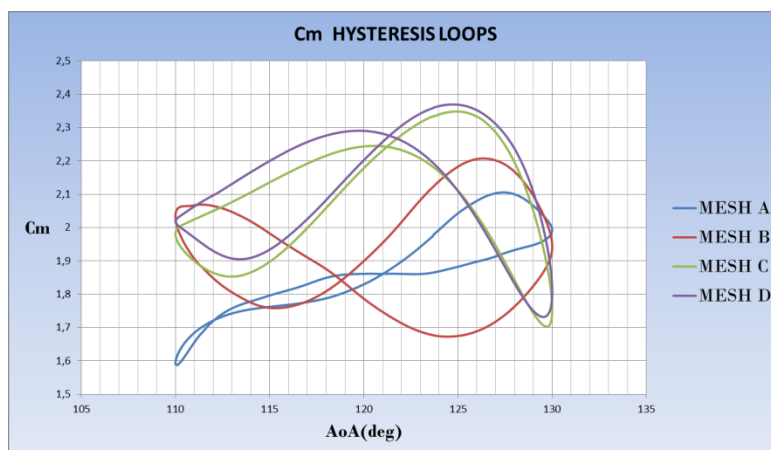


Figure 10: (Mesh sensitivity for moment coefficient hysteresis loop)

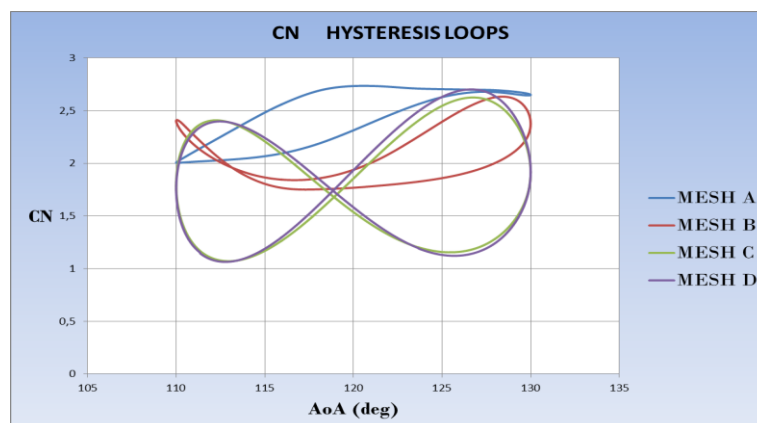


Figure 11: (Mesh sensitivity for normal force coefficient hysteresis loop)

The loops obtained with Mesh C and Mesh D present a very similar shape and a crossing point that occurs for α slightly greater than 120° (that is the equilibrium configuration). The other two loops are very different, proving that those results are far from being grid independent.

4.3 Time Step Sensitivity Analysis

A sensitivity analysis with respect to time step size is important in order to evaluate whether the aerodynamic time-dependent phenomena are adequately represented by CFD. The input parameters (that is motion frequency and Mach number) are the same used for the mesh sensitivity analysis, with the exception of time step size which is varied; MESH C is adopted for calculations. The cases investigated are reported in Table 4.

Table 4: Adopted time step sizes, $\omega=0.5$ rad/s, $M_\infty=0.6$

Case	dt (s)
A	0.1
B	0.01
C	0.001

For each case the time histories of the aerodynamic coefficients are compared as well as the hysteresis loops, as reported in Fig. 12 and 13.

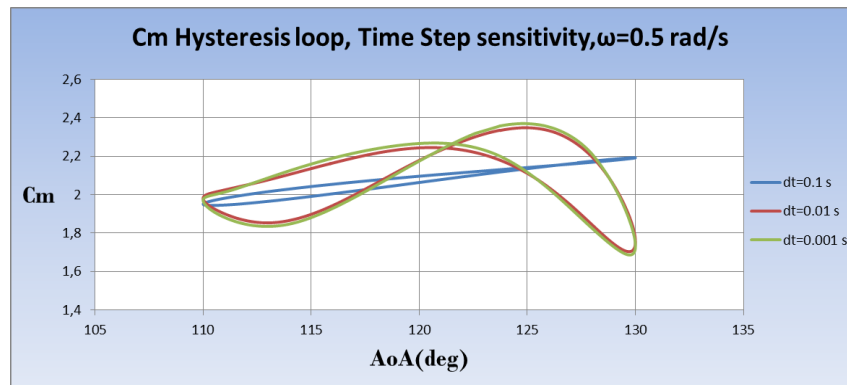


Figure 12: Time step sensitivity for C_m hysteresis loops for $\omega=0.5$ rad/s, $M_\infty=0.6$, MESH C

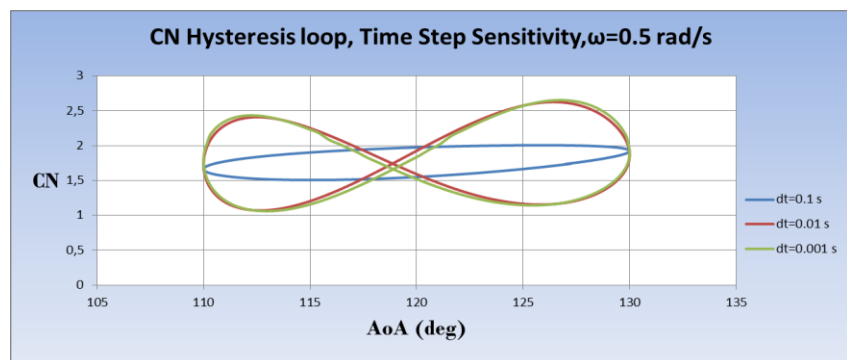


Figure 13: Time step sensitivity of normal coefficient for $\omega=0.5$ rad/s, $M_\infty=0.6$, MESH C

The sensitivity analysis with respect to the time step shows that the differences between CASE B ($dt=0.01$ s) and CASE C ($dt=0.001$ s) are very small: the hysteresis loops are very similar and the difference in terms of the computed dynamic derivatives is less than 1%.

4.4 Aerodynamic damping evaluation by means of CFD

A parametric analysis with respect to angular velocity ω has been performed, keeping the Mach number fixed. The aim is to understand how the aerodynamic damping is influenced by the frequency of motion. All simulations have been performed using the Fluent setup illustrated in Section 3.4, MESH C (3.8 million cells) and time step size equal to 0.01 s. Figure 14 (a) reports the dependence of C_{mEQ} on frequency for a fixed M and Figure 14 (b) includes in the same plot the hysteresis loops at different frequencies but at the same M.

It is clearly observed that the aerodynamic damping C_{mEQ} is strongly influenced by the frequency of motion. A peak (in absolute value) is present in the range in between 0.1 rad/s and 0.5 rad/s , while, as ω increases, the damping shows an asymptotic trend, settling around a value of about -20 rad^{-1} . The hysteresis loops for C_m become larger as the frequency increases, engulfing the ones corresponding to slower motions. All the hysteresis loops (relative to moment coefficient) are run counter-clockwise, confirming that the damping is negative in the sense that energy is being dissipated. This can also be explained analytically [5]: for sinusoidal oscillations the plot of $\dot{\alpha}(t)$ vs. $\alpha(t)$ is a clockwise loop since it is just like the plot of $\cos \omega t$ vs. $\sin \omega t$. As immediate consequence the plot of $-\dot{\alpha}(t)$ vs. $\alpha(t)$ is counterclockwise. The pitch moment coefficient can be written as

$$C_m = C_m(\alpha) + C_{mq}\hat{q} + C_{m\dot{\alpha}}\hat{\alpha}$$

With the assumption that $q = \dot{\alpha}$ and introducing the definition of C_{mEQ} one obtains:

$$C_m = C_m(\alpha) + C_{mEQ}\hat{\alpha}$$

If C_{mEQ} is negative, for what was said above the resulting hysteresis loops are necessarily counter-clockwise. It is then possible to notice how the shape of the loops is also deeply influenced by the frequency: for intermediate frequencies (around 1 rad/s) the loops are “eight shaped” whereas for higher or lower frequencies they resemble ellipsis. This can be explained if one considers the time histories of aerodynamic coefficients corresponding to intermediate, a secondary frequency appears in addition to the main one determining more irregular oscillations of the coefficients.

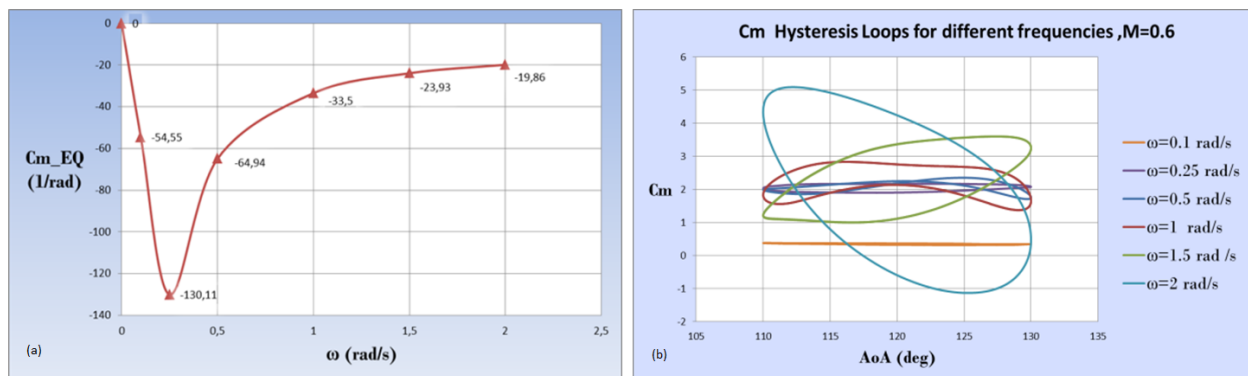


Figure 14: (a) Dependence of C_{mEQ} on frequency for $M=0.6$, (b) Dependence of moment coefficient hysteresis loops on frequency, $M=0.6$

4.4 Aerodynamic damping evaluation by means of Datcom

MISSILE DATCOM is a widely-used semi-empirical code for the preliminary design of missile and aircraft aerodynamic performance. It is able to provide accurate results in terms of aerodynamic coefficients for several flow conditions and body geometries. The code is also able to compute longitudinal stability derivatives according to the Slender Body Theory discussed above. It is therefore interesting to compare CFD results with DATCOM predictions. In order to have coherent results the reference quantities in the DATCOM input file must be set equal to the ones defined in Fluent, that is the body base diameter and cross section.

The computed derivatives do not depend upon the angle of attack as expected since DATCOM method is based on slender body theory. In particular DATCOM computes the derivatives in conditions of angle of attack near zero [6]. Another important limitation is that the dependence of pitch damping coefficients on reduced frequency cannot be

predicted: the method used by DATCOM for calculating dynamic derivatives can be applied only to slow time dependent motions.

The derivatives computed with DATCOM are summarized in Table 5, and it is shown that differences with respect to CFD results (performed with ω (rad/s)=0.25, $\alpha_{\text{mean}}=120^\circ$ and $M=0.6$) reaches values of about 96%.

Table 5: Dynamic derivatives computed with MISSILE DATCOM

Derivatives (1/rad)	DATCOM
C_{mEQ}	-4.64

Nevertheless when the angle of attack is close to zero DATCOM should instead represent an accurate way to estimate the pitch damping coefficient. The comparison between DATCOM results and CFD predictions at small angles of attack has been evaluated through another CFD simulation. The study has been carried out by imposing a sinusoidal motion around $\alpha_{\text{mean}}=0^\circ$ instead of $\alpha_{\text{mean}}=120^\circ$, and keeping Mach number constant and equal to 0.6. The frequency of motion is equal to a relatively small value, here set to 0.25 rad/s (~ 15 deg/s). In this configuration, the hypothesis of slender body theory are certainly respected. Table 6 reports the difference between CFD and Datcom results whereas the hysteresis loop and Mach contour plot computed for $\alpha_{\text{mean}} = 0$ are reported in Figure 15.

Table 6: Dynamic derivatives computed with MISSILE DATCOM

Derivatives (1/rad)	DATCOM	CFD	Difference (%)
C_{mEQ}	-4.64	-4.31	7%

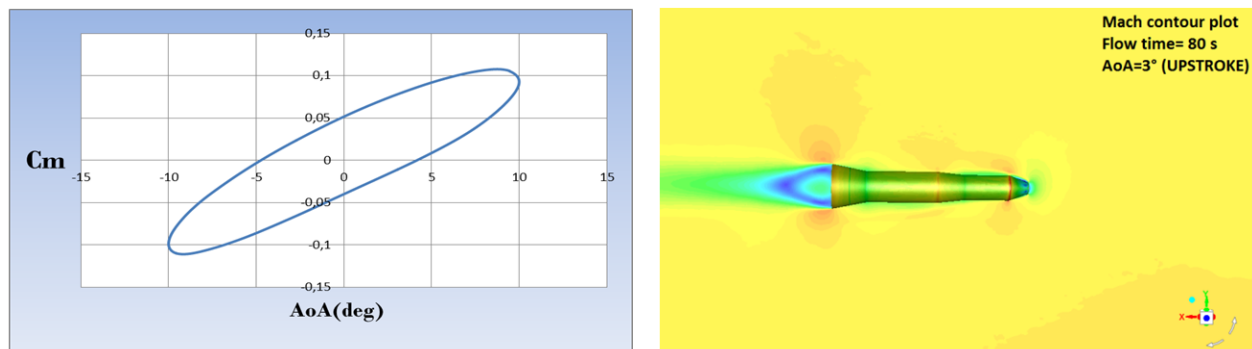


Figure 15: Hysteresis loop and Mach contour plot for $\alpha_{\text{mean}} = 0$ and $M=0.6$.

5. Conclusions

3D unsteady CFD simulations have been performed with the aim of evaluating the pitch damping aerodynamic coefficients in a free fall condition. Forced oscillations around an equilibrium position ($\alpha_{\text{mean}}=120^\circ$) have been imposed to the body. The Mach number has always been set equal to 0.6. A mesh sensitivity analysis has been conducted and revealed that using a mesh made up of 3.8 million cells and containing a minimum cell size (close to the body surface) of 0.05 m leads to accurate results, with a difference lower than 2% on the computed quantities. A sensitivity analysis with respect to the time step has been performed as well and proved that a time step size of 10^{-2} s is adequate to correctly reproduce the unsteady phenomena. No appreciable difference is found in the comparison with the same analysis using a time step equal to 10^{-3} s: the difference in terms of pitch damping coefficient is less than 1% and the shape of hysteresis loops results very similar.

The functional trend of pitch aerodynamic coefficients with respect to reduced frequency in the range $k = [0.048 ; 0.957]$ has been investigated: a peak in absolute value is found for a value of reduced frequency equal to 0.119 ($\omega=0.25$ rad/s) and an asymptotic trend as ω increases. This analysis has shown a strong influence of motion frequency on damping coefficients, this mainly due to non linear aerodynamics at high angles of attack.

As a further element of discussion, comparisons with MISSILE DATCOM have been made. Large differences (up to 90%) have been found for the case with $\alpha_{\text{mean}}=120^\circ$ due to the fact that DATCOM method is based on the slender body theory, thus it is not able to provide reliable results for high angles of attack and high frequencies of motion. However, for low angles of attack and relatively slow time-dependent motions DATCOM predictions are found to be in good agreement with CFD results and literature reference outcomes.

References

- [1] Munk, M.M., "The aerodynamic forces on Airship hulls", NACA Report N.184, 1924.
- [2] Tsien, H.S. , "Supersonic Flow Over an Inclined Body of Revolution", Journal of Aeronautical Science ,5,pp.480-483,1938.
- [3] Multhopp, H. , "Aerodynamics of the Fuselage", NACA TM 1036, 1942.
- [4] Allen, H.J., "Estimation of the Forces and Moments Acting on Inclined Bodies of Revolution of High Fineness Ratio", NACA RM A9126,1949.
- [5] Yigang F., "Identification of an Unsteady Aerodynamic model up to high angles of attack ", Faculty of Virginia Polytechnic Institute and State University, November 1997, Blacksburg, Virginia
- [6] Blake ,B. W., "MISSILE DATCOM USER'S MANUAL"-1997 FORTRAN 90 REVISION , Fink.R, Guide to DATCOM and methods summary ,McDonnell Douglas Corporation-Douglas Aircraft Division, Long Beach, California, April 1978.
- [7] Da Ronch, A., Vallespin, D., Ghoreyshi, M., and Badcock, K. J., "Computation of Dynamic Derivatives Using CFD," 28th AIAA Applied Aerodynamics Conference, AIAA Paper 2010-4817, June–July 2010.
- [8] Bhagwandin, V., and Sahu, J., "Numerical Prediction of Pitch Damping Stability derivatives for Finned Projectiles", Journal of Spacecraft and Rockets, Vol. 51, No. 5, 2014.
- [9] McGowan, G.Z., Kurzen, M.J., Nance, R.P. and Carpenter, J.G. "High Fidelity Approaches for Pitch Damping Prediction at High Angles of Attack", Journal of Spacecraft and Rockets, Vol. 51, No. 5, 2014.